0026-895X/91/020242-06$03.00/0
Copyright © by The American Society for Pharmacology and Experimental Therapeutics
All rights of reproduction in any form reserved.
MOLECULAR PHARMACOLOGY, 40:242–247

MOL PHARM

Functional Responses of Cloned Muscarinic Receptors Expressed in CHO-K1 Cells

S. V. PENELOPE JONES,[1] CRAIG J. HEILMAN, and MARK R. BRANN[1]

Laboratories of Biophysics (S.V.P.J.), Neurophysiology (S.V.P.J.), and Molecular Biology (S.V.P.J., C.J.H., M.R.B.), National Institute of Neurological Disorders and Stroke, National Institutes of Health, Bethesda Maryland 20892, and Neuroscience Research Unit, Department of Psychiatry (S.V.P.J., M.R.B.), University of Vermont College of Medicine, Burlington, Vermont 05405

Received August 13, 1990; Accepted May 9, 1991

SUMMARY

The physiological responses to activation of the m5 muscarinic acetylcholine receptor were compared with those of m3 and m4 in transformed Chinese hamster ovary cells, using patch-clamp electrophysiological and biochemical techniques. Stimulation of the m5 receptor induced increases in both a calcium-dependent potassium conductance and phosphoinositide (PI) metabolism of similar magnitude to those activated by m3. Raising of intracellular calcium or injection of inositol-1,4,5-trisphosphate mimicked the activation of the calcium-dependent potassium conductance by both of these receptors. Although similar regarding these responses, the m3 and m5 receptors induced different cAMP responses. Stimulation of m5 receptors induced a 2-fold increase in cAMP levels, whereas m3 induced a 20-fold increase. These cAMP responses required >100-fold more agonist than the PI responses, and both PI and cAMP responses were insensitive to pertussis toxin. Stimulation of m4 receptors caused little increase in PI metabolism and no electrophysiological effects. Stimulation of m4 receptors with low concentrations of agonist decreased cAMP levels, but at high agonist concentrations cAMP levels were elevated. After treatment with pertussis toxin, the decrease in cAMP levels induced by m4 was blocked and a marked increase in cAMP levels, comparable to those observed for m3 receptors, was uncovered at higher doses. The data indicate that each of the receptors has distinct functional properties.

The genes encoding five muscarinic ACh receptor subtypes have been cloned (m1–m5) (1–5). The functional properties of each of these subtypes were examined after their expression in transformed cell lines. Physiological data have shown that m1 and m3 inhibit the m-current and can activate calcium-dependent potassium and chloride conductances (6–8). The activation of the calcium-dependent conductances is thought to be due to release of calcium by IP_3 (9, 10). This is supported by the demonstration of an enhancement of PI metabolism upon stimulation of m1 or m3 (11–13). Further biochemical analysis showed that m1 and m3 also modestly increased cAMP levels in A9 L (11, 14) and HEK cells (13). This increase in cAMP in A9 L cells is thought to be mediated indirectly by the rise in intracellular calcium concentration that results from stimulation of phospholipase C (15).

m2 and m4 muscarinic receptor subtypes have not demonstrated any electrical response in transformed cell lines to date but have been shown to decrease cAMP levels (13, 14, 16). The actions of m5 have not been directly compared with those of the other receptor subtypes, but initial data suggest that m5 may be similar to the m1 and m3 subtypes, because it also activated PI metabolism (5, 17). The present study investigates the electrophysiological and biochemical actions of m5 in CHO cells and compares them with those of m3 and m4 in these cells.

Materials and Methods

Tissue culture. The m3-, m4-, and m5-transformed CHO cells of this study have been described previously (18). As assessed by *N*-[^{3}H] methylscopolamine binding, the receptor levels were 2.0, 0.9, and 2.2 pmol/mg of protein for m3-, m4-, and m5-transformed cells, respectively (18). No detectable muscarinic receptor binding sites were demonstrated in nontransformed CHO cells. Cells were incubated at 37° in 5% CO_2, in Dulbecco's modified Eagle medium with 10% fetal calf serum, 100 units/ml penicillin, 100 μg/ml streptomycin, 1% proline, and 2 mM glutamine, for at least 24 hr before electrophysiological recordings or biochemical assay.

Patch-clamp techniques. Cells were studied at room temperature (21–23°) on the inverted stage of a phase contrast microscope, at a magnification of 320×. The whole-cell patch-clamp recording technique was used to record membrane currents and potentials, using a LIST

[1]Present address: Neuroscience Research Unit, Department of Psychiatry, Medical Alumni Building, University of Vermont, Burlington, VT 05405.

ABBREVIATIONS: ACh, acetylcholine; PI, phosphoinositide; CHO, Chinese hamster ovary; IP_3, inositol 1,4,5-trisphosphate; HEPES, 4-(2-hydroxyethyl)-1-piperazineethanesulfonic acid; EGTA, ethylene glycol bis(β-aminoethyl ether)-*N,N,N′,N′*-tetraacetic acid; PTX, pertussis toxin; IP_1, inositol monophosphate; BAPTA, 1,2-bis(2-aminophenoxy)ethane-*N,N,N′,N′*-tetraacetic acid.

MOLECULAR PHARMACOLOGY
aspet
Downloaded from molpharm.aspetjournals.org at Universidade do Estado do Rio de Janeiro on December 4, 2012

MOL PHARM

MOLECULAR PHARMACOLOGY

EPC-7 amplifier (19). The patch electrodes were made from thin-wall capillary borosilicate glass (World Precision Instruments, New Haven, CT) and pulled on a two-stage horizontal electrode puller (Mecanex, Basel, Switzerland). Pipette resistances were about 5 MΩ. Pipette seals of 5–20 GΩ were obtained before disruption of the patch. After patch rupture, input resistances of 0.5–1 GΩ were obtained at resting potentials. Series resistance compensation was applied in voltage clamp.

The ionic composition of the extracellular medium was (in mM) 140 NaCl, 5 KCl, 5.6 glucose, 2 $CaCl_2$, and 1 $MgCl_2$, pH adjusted to 7.4 with NaOH. The osmolarity was adjusted to 330–335 mOsM with sucrose. The intracellular patch pipette solution contained (in mM) 150 potassium gluconate, 2 $MgCl_2$, 5 HEPES, 1.1 EGTA, 0.1 $CaCl_2$, 5 Mg-ATP, and 0.1 Li-GTP, pH adjusted to 7.2 with KOH. The osmolarity was adjusted to 320–325 mOsM. The free intracellular calcium concentration was about 20 nM (20).

Liquid-junction potentials between the bath solution and the intracellular electrode were eliminated by filling a side bath containing the reference electrode with the intracellular solution. Connections between the two baths were made via a low-resistance agar bridge.

Membrane currents were recorded from cells voltage-clamped at −50 mV. Either resting current measurements were taken or the currents produced by a series of hyperpolarizing and depolarizing voltage steps were recorded. ACh (10–50 μM) was applied by low pressure (1–2 psi) from a micropipette placed close to the cell. The current and voltage responses were displayed on a Gould pen recorder (filtered at 50 Hz) and also sampled and digitized on-line by a PDP 11/23 minicomputer with an analog-to-digital Data Translation converter (12 bit, ± 5 V range), at a digitization rate of 2.5 kHz. Signals were filtered at 1 kHz. Antagonists were applied directly to the bath, and solution changes were obtained by perfusion of the 1.5-ml bath (21) with fresh medium at a flow rate of 2 ml/min. All results are expressed as mean ± standard error.

cAMP assay. cAMP levels were measured by automated radioimmunoassay, using the Gammaflow system, against a standard curve ranging from 0.78 to 50 pmol/ml acetyl-cAMP. Assays were performed on nonconfluent monolayers grown in 24-well plates, by first washing the cells with Earle's minimal essential medium, containing 20 mM HEPES, 0.5 mM $CaCl_2$, 1 mM $MgCl_2$, and 1 mM isobutylmethylxanthine, and then exposing them to agonist in this solution for 10 min at 22°. In experiments with m4, 1 μM forskolin was added to the incubation medium to raise the intracellular cAMP levels. The reaction was quenched by addition of 0.1 M HCl plus 0.1 mM $CaCl_2$. The cAMP of the standards and samples was acetylated by addition of a mixture of 70% triethylamine and 30% acetic anhydride. Data are representative of two or three independent experiments performed in duplicate, expressed as mean ± standard error.

PI assay. Phosphatidyl inositol hydrolysis was measured by preincubating cells in 24-well plates for 2 days with 0.5 μCi of *myo*-[^{3}H] inositol in growth medium. The cells were then washed with Earle's minimal essential medium containing 25 mM HEPES and 0.1 mM LiCl and were exposed to agonist for 60 min at 22°. The reaction was terminated by addition of 10% trichloroacetic acid and subsequently extracted with water-saturated diethyl ether, neutralized, and passed over Dowex anion exchange resin to isolate inositol phosphate fractions. Results are representative of two or three independent experiments expressed as mean ± standard error.

Drugs. ACh chloride, apamin, carbamylcholine chloride, 3-isobutyl-1-methylxanthine, atropine sulfate, and 8-bromo-cAMP (Sigma Chemical Co., St. Louis, MO); BAPTA (Molecular Probes, Eugene, OR); PTX (List Biological Laboratories, Campbell, CA); lithium IP_3 and forskolin (Calbiochem, San Diego, CA); ^{125}T-cAMP and acetyl-cAMP antibody (Dr. G. Brooker, Georgetown University, Washington, DC); and *myo*-D-[^{3}H]inositol (NEN-Dupont) were obtained from the indicated sources.

Results

Electrophysiology of m5-transformed CHO cells. The membrane potential of CHO cells on first breaking into the whole-cell mode was −55 ± 3 mV (n = 19) in m5 transformants and −52 ± 3 mV (n = 17) and −53 ± 3 mV (n = 18) in m3- and m4-transformed cells, respectively. Resting conductances were 1.5 ± 0.5 nS (n = 11) in m5-transformed cells, 1.2 ± 0.3 nS (n = 11) in m3-transformed cells, and 1.1 ± 0.2 nS (n = 13) in m4-transformed cells. Upon application of ACh (10–50 μM), outward currents were observed in m3- and m5-transformed cells, when the cells were voltage-clamped at −50 mV. Whole-cell conductances were increased approximately 3-fold over resting levels in the presence of ACh in both m3 and m5 cell lines, increasing to 2.8 ± 0.5 nS (n = 11) in m3- and 3.2 ± 0.8 nS (n = 11) in m5-transformed cells. The current-voltage relationship for m5, obtained by stepping the membrane potential from −50 mV to a variety of potentials for 100 msec, is shown in Fig. 1, in the absence and presence of ACh. ACh was applied for the duration of the current-voltage curve (~25 sec). Continued application of ACh beyond this period resulted in a decline in the response. The ACh-induced equilibrium potential was −67 ± 3 mV (n = 5). This conductance increase was associated with a hyperpolarization of the cell membrane of about 15 mV, from −55 mV to −70 mV (n = 2). Application of ACh to m4-transformed cells had no effect on the membrane properties of the CHO cell (n = 22).

Comparison of conductances activated in m3- and m5-transformed cells. In m5-transformed cells, the ACh-induced conductance was largely dependent on potassium, as demonstrated by the shifting of the equilibrium potential 45 mV, from −67 ± 4 mV (n = 4) in 5 mM KCl (E_K = −86 mV) to −22 ± 2 mV (n = 4) in 50 mM KCl (E_K = −28 mV). This was very similar to that found in m3-transformed cells, where the equilibrium potential was shifted 46 mV, from −66 ± 5 mV (n = 5) to −20 ± 5 mV (n = 5), on increasing of the extracellular KCl from 5 to 50 mM. Thus, m3 and m5 appear to have an equal dependence on K^+. The dependence of the m5 response on K^+ concentration is shown in detail in Fig. 2, demonstrating a 50-mV change in potential/10-fold change in K^+ concentration. Ion substitution experiments discounted the involvement of Cl^- or cation conductances in the muscarinic receptor-induced response. In recordings with 150 mM *N*-methylglucamine methyl sulfonate in the patch pipette substituted for potassium gluconate, no current responses were detectable upon applica-

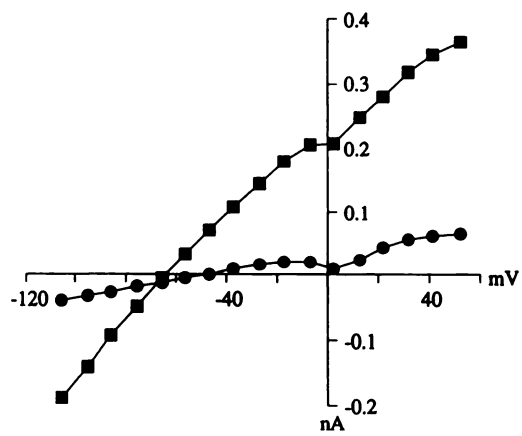

Fig. 1. Representative current-voltage relationship for control (●) and ACh-induced (■) whole-cell conductance in m5-transformed CHO cells. Currents were measured 10 sec after the onset of the 100-msec step. Resting slope conductance for this cell was 0.8 nS, which increased to 3.6 nS upon application of 10 μM ACh. The polarity of the ACh-induced conductance (E_{ACh}) reversed at −65 mV in this cell.

Downloaded from molpharm.aspetjournals.org at Universidade do Estado do Rio de Janeiro on December 4, 2012

aspet

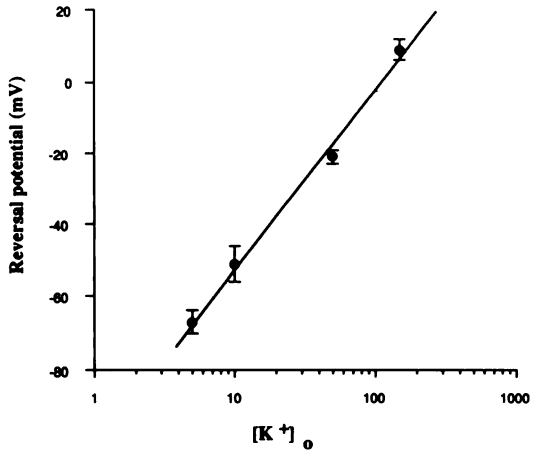

Fig. 2. Effects of extracellular K^+ on the reversal potential of ACh-induced currents. Data indicate mean ± standard error (n = 4). *Solid line*, best fit to the data, with a slope of 50 mV/10-fold change in K^+ concentration.

tion of ACh either in an extracellular solution containing (in mM) 145 N-methyl glucamine chloride, 2 $CaCl_2$, 1 $MgCl_2$, 5 HEPES, and 5.6 glucose (n = 4) or in a solution containing (in mM) 145 sodium methyl sulfonate, 2 $CaCl_2$, 1 $MgCl_2$, 5 HEPES, and 5.6 glucose (n = 4), although ACh could activate conductance increases when these cells were bathed in a solution containing (in mM) 150 KCl, 2 $CaCl_2$, 1 $MgCl_2$, 5 HEPES, and 5.6 glucose. The difference between the experimental E_{ACh} and the calculated E_K is probably due in part to the liquid-junction potential between the pipette solution and the physiological intracellular composition of the cell and in part to the incomplete dissociation of potassium gluconate in solution.

A comparison of the pharmacology of the ACh-induced responses is shown in Figs. 3 and 4. Atropine blocked both responses at a concentration of 1 μM, showing them both to be mediated by muscarinic receptors. Cobalt (5 mM), a calcium channel-blocking agent, attenuated the ACh-induced responses in both m3 and m5 transformants. The mechanism of action of cobalt is unknown but may be due to competition with Ca^{2+} for the binding site at the K^+ channel. Barium (5 mM), a potassium channel blocker, and apamin (0.5 μM), a calcium-dependent potassium channel-blocking agent, also inhibited the ACh-induced responses of m3 and m5. In experiments in which the buffering of released intracellular calcium was increased in comparison with solutions used in the remainder of the study (n = 77), by addition of 5 mM BAPTA to the intracellular solution, current responses evoked by ACh were prevented (n = 12), further establishing the calcium-dependent nature of the response. Therefore, stimulation of both the m3 and m5 muscarinic receptor subtypes resulted in activation of calcium-dependent potassium conductances, as demonstrated earlier for m1 and m3 in A9 L cells (7, 8).

Lack of effect of m3, m4, or m5 on sodium current. From the control current-voltage (I-V) curve for m5-transformed cells shown in Fig. 1, it was observed that the CHO cell contained evidence of a small voltage-sensitive conductance, which activated at around −20 mV, peaked at around 0 mV, and reversed polarity close to +40 mV. Leak subtraction of the I-V curve revealed this conductance in more detail and showed that it was dependent on sodium and could be abolished by application of 1 μM tetrodotoxin to the bath, indicative of a

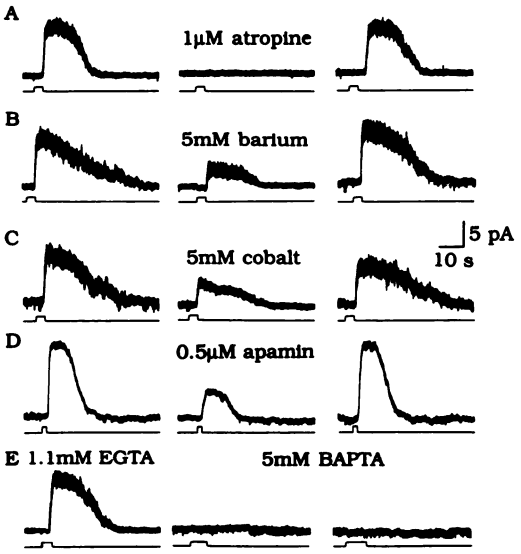

Fig. 3. Traces show currents activated by application of 10–50 μM ACh in m5-transformed cells voltage-clamped at −30 or −50 mV. A, 1 μM atropine; B, 5 mM barium; C, 5 mM cobalt; D, 0.5 μM apamin. *Left*, control responses; *center*, responses recorded about 5 min after addition of the agent to the bathing medium; *right*, recovery response after drug washout. E, Responses to ACh from two different cells. *Left*, cell recorded with a pipette containing 1.1 mM EGTA (used in all other experiments); *center* and *right*, no response to ACh after increasing of intracellular calcium buffering by addition of 5 mM BAPTA to the intracellular patch pipette solution. The upward deflections of the lower traces in each panel show the application of ACh from a pressure ejection pipette.

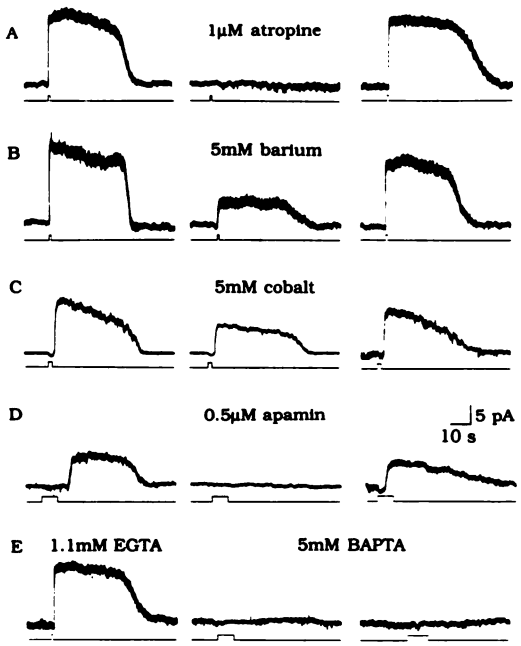

Fig. 4. Traces of ACh-induced currents from m3-transformed cells voltage-clamped at −30 or −50 mV. ACh (50 μM) was applied by pressure ejection pipette. A–D, *Left*, control responses; *center*, responses after addition of drug to the bathing medium; *right*, recovery. Atropine (1 μM) (A), barium (B), cobalt (C), and apamin (D) all attenuate the ACh-induced currents. E, Responses to ACh from two different cells. *Left*, cell recorded with a pipette containing 1.1 mM EGTA; *center* and *right*, no response to ACh after addition of 5 mM BAPTA to the intracellular solution. The upward deflections of the lower traces in each panel denote the application of ACh.

MOL PHARM
MOLECULAR PHARMACOLOGY
aspet
Downloaded from molpharm.aspetjournals.org at Universidade do Estado do Rio de Janeiro on December 4, 2012

MOL PHARM

MOLECULAR PHARMACOLOGY

sodium current. Neither the m3, the m4, nor the m5 muscarinic receptor subtype appeared to effect this sodium current.

Actions of m3, m4, and m5 on PI metabolism. Nontransformed CHO cells displayed no significant changes in PI metabolism in response to carbachol treatment (data not shown). The dose-response curves for increasing concentrations of carbachol are shown plotted against fold increases in IP_1, relative to basal levels (Fig. 5), for m3-, m4-, and m5-transformed CHO cells. Basal levels of IP_1 were 99 ± 8 cpm/well (n = 6). Stimulation of both m3 and m5 muscarinic receptors resulted in increases in PI metabolism. m3 increased IP_1 12.6 ± 3.8-fold (n = 3) over basal levels, with an ED_{50} of ~2 μM. m5 increased IP_1 levels by 15.9 ± 5.7-fold (n = 3) over baseline, with an ED_{50} of ~400 nM. Neither response to agonist was significantly affected by incubation with PTX (100 ng/ml overnight). m4 either produced no detectable effect on PI metabolism (with or without PTX preincubation) or stimulated a very small rise in IP_1, which was too small (<2-fold) for accurate determinations.

Actions of m3, m4, and m5 on cAMP levels. Nontransformed CHO cells displayed no significant changes in cAMP levels in response to carbachol treatment (data not shown). The dose-response curve of carbachol-stimulated effects on cAMP levels is shown in Fig. 6A for m3-, m4-, and m5-transformed cells. Basal cAMP levels were estimated to be 3.7 ± 0.6 pmol/ml (n = 5) (each well contained 0.5 ml). Stimulation of m3 by carbachol resulted in a 19.4 ± 3.5-fold (n = 4) increase in cAMP levels. The ED_{50} for this response was >200 μM. The maximal response was not ascertained, even using carbachol concentrations as high as 2 mM. m5, on the other hand, produced a minor increase in cAMP levels over basal, just 2.3 ± 0.7-fold (n = 3). The ED_{50} of this response was >200 μM. PTX (100 ng/ml overnight) had a slight effect in reducing the peak cAMP responses to m3. It is very clear from Fig. 6A that m3 produced a dramatic stimulation of cAMP, compared with m5.

The dual effects of m4 stimulation on cAMP levels are shown in Fig. 6A. The inhibition of cAMP is shown at greater resolution in Fig. 6B. Basal concentrations of cAMP after forskolin stimulation were 9.3 ± 0.9 pmol/ml cAMP (n = 5). Low concentrations of carbachol, from 10 nM to 1 μM, inhibited the forskolin-induced rise in cAMP, with an ED_{50} of 25 nM. However, higher concentrations than this resulted in a dose-dependent increase in cAMP, denoted by the upward turn of the dose-response curve. This increase in cAMP levels can be seen more clearly (Fig. 6A) after PTX treatment (100 ng/ml overnight). The PTX treatment completely abolished the inhibitory component of m4 on cAMP levels and thus revealed the PTX-insensitive increase in cAMP. The m4-stimulated increase in cAMP levels was 12.7 ± 2.4-fold (n = 3) over baseline and had an ED_{50} of ~5 μM. In two other independently m4-transformed CHO cell lines, carbachol both decreased cAMP levels (30–40%; ED_{50}, <100 nM) and increased cAMP levels (ED_{50}, ~5 μM) at higher doses (data not shown).

Unfortunately, m1- and m2-transformed CHO cells that express receptors at levels comparable to those of the m3 and m5 transformants were not available for this study (0.1–0.2 versus 0.9–2 pmol/mg of protein). Thus, their response properties cannot be directly compared. In these low level m1-transformed cells, carbachol increased IP_1 levels >10-fold (ED_{50}, ~10 μM). Little effect on cAMP levels was observed (<2-fold increase). In these low level m2-transformed cells, carbachol decreased basal (ED_{50}, ~1 nM) and forskolin-stimulated

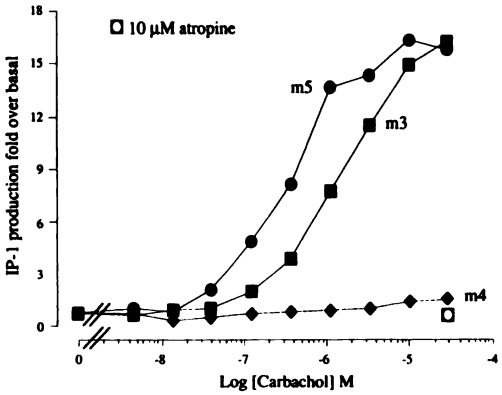

Fig. 5. Effects of carbachol on IP_1 levels in m3-, m4-, and m5-transformed cells. Similar numbers of CHO cells transformed with m3, m4, and m5 were incubated for 1 hr with a range of concentrations of carbachol, the resultant production of IP_1 was measured, and a dose-response curve was constructed. In this experiment, m5 (●) produced an increase in IP_1 levels with an ED_{50} of ~500 nM. m3 (■) produced an increase in IP_1 with an ED_{50} of ~1.5 μM. m4 (♦) had very little effect on IP_1 levels. Atropine (10 μM) blocked all responses to carbachol.

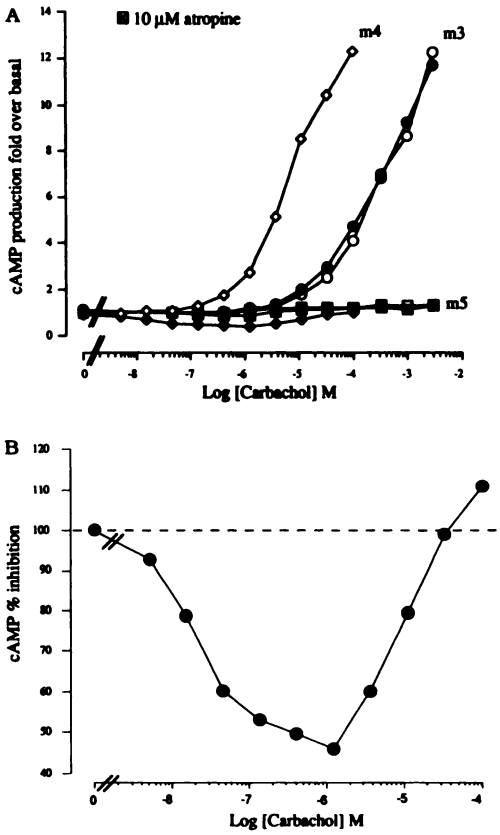

Fig. 6. Effects of carbachol on cAMP levels in m3-, m4-, and m5-transformed cells. Similar numbers of CHO cells transformed with m3, m4, and m5 receptor subtypes were incubated with a range of carbachol concentrations. A, cAMP levels for m3 (*circles*), m4 (*diamonds*), and m5 (*squares*) in the presence (*open symbols*) and absence (*closed symbols*) of PTX (100 ng/ml). The maximal stimulation of cAMP levels by m3 was not reached even at 3 mM and, thus, the ED_{50} for the m3 response could only be approximated to >200 μM. The m4-induced increase in cAMP in cells preincubated with PTX had an ED_{50} of ~6 μM in the experiment shown. B, m4-induced reduction in cAMP formation in the absence of PTX treatment. Carbachol (1 μM) maximally inhibited forskolin-induced cAMP formation by 45%, with an ED_{50} of 30 nM. Carbachol concentrations above 1 μM resulted in a dose-dependent upward deflection of the curve. Atropine (10 μM) inhibited all responses.

Downloaded from molpharm.aspetjournals.org at Universidade do Estado do Rio de Janeiro on December 4, 2012

aspet

MOL PHARM

cAMP levels by 40 and 36%, respectively. No effect was observed on IP_1 levels, and high agonist doses did not increase cAMP levels (data not shown). After completion of this study, m1 CHO cells expressing 2 pmol/mg of protein were isolated. In these cells, carbachol induced a >10-fold increase in cAMP levels (ED_{50}, >200 μM).

Mimicry of the electrical response of m5 by IP_3 and lack of effect of cAMP. Inclusion of 100 μM IP_3 in the patch pipette resulted in activation of outward currents ($n = 4$) at −50 mV upon rupture of the patch into the whole-cell mode (Fig. 7), similar to those activated by ACh in m5-transformed cells. Control experiments showed no change in holding current upon breakthrough into the whole-cell mode ($n = 61$). Increasing of the intracellular free calcium concentration to 1 μM (1.1 mM EGTA plus 1 mM Ca^{2+}) also activated outward currents at −50 mV ($n = 3$), again mimicking the m5 ACh-induced response. Application of 5 mM 8-bromo-cAMP to the cell from a second pressure ejection pipette had no effect on resting membrane properties and, therefore, did not appear to mimic the ACh-induced response.

Discussion

In the present study, the m3 and m5 receptors shared functional properties such as activation of a calcium-dependent potassium conductance and stimulation of PI metabolism. The magnitudes of the conductance and IP_1 increases were similar for both m3 and m5. The activation of the potassium conductance increase by m5 was mimicked in CHO cells by IP_3 and by raised intracellular free calcium, which is consistent with channel opening being mediated by IP_3-induced release of calcium from intracellular stores. This mechanism has been previously worked out for m1 and m3 in A9 L cells (10). m4 had no electrically detectable effect on the CHO cell membrane and produced a negligible PI stimulation. Thus, the m1, m3, and m5 receptors are similar in their coupling to phospholipase C, with subsequent opening of calcium-dependent channels.

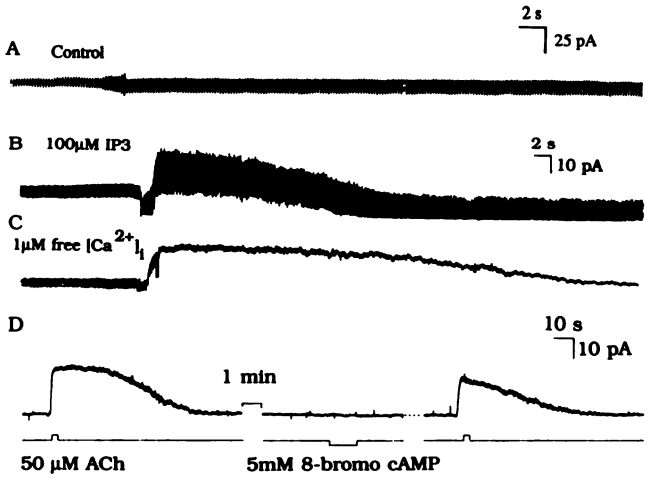

Fig. 7. Traces show currents recorded from m5-transformed CHO cells initially in cell-attached patch mode, to show the rupture of the patch to the whole-cell mode. Cells were voltage-clamped at −50 mV. A, Control. B, Inclusion of 100 μM IP_3 in the patch pipette resulted in an outward current response associated with an increase in conductance. C, Increasing the intracellular free calcium concentration to 1 μM resulted in activation of the outward current response on breaking through the patch into the whole-cell mode. D, Application of ACh from a pressure ejection pipette (upward deflection of the lower trace) activated the calcium-dependent potassium conductance in an m5-transformed cell whole-cell voltage-clamped at −50 mV (*left*). Application of 8-bromo-cAMP from a second pressure ejection pipette (downward deflection in lower trace) had no effect on the cell membrane (*center*). Response to ACh after application of 8-bromo cAMP (*right*).

Previously, m1, m3, and m5 have been classed together by function (stimulating phospholipase C), as had m2 and m4 (inhibiting adenylate cyclase). In the case of the m5 receptor, this assignment was somewhat tenuous, because it had not been directly compared with the other receptors using similar cells and levels of expression (5, 17). Our PI and channel data confirm this functional division (m3 and m5 versus m4), whereas our cAMP data do not. m3 and m4 (in the presence of PTX) strongly increase cAMP levels, whereas m5 does not. The cAMP responses reported here are unlike those that have been previously reported in A9 L (14) and HEK (13) cells. In A9 L cells transformed with m1 and m3 receptors, we previously observed modest elevations in cAMP levels and PI hydrolysis, which had identical dose-response relationships. Only a PTX-sensitive decrease in cAMP levels was previously observed in the m4-transformed A9 L cell (12, 14). These and other data have suggested that the cAMP elevations are due to activation of adenylate cyclase by a calcium-dependent mechanism (secondary to PI metabolism) (15). The present results suggest no correlation with PI hydrolysis. m3 and m4 (in the presence of PTX) had equivalent effects on cAMP levels, whereas m4 had little or no effect on PI hydrolysis. m3 and m5 had similar effects on PI hydrolysis, whereas m5 had much less effect on cAMP levels. Finally, the dose-response relationships of the effects on PI hydrolysis and cAMP levels differed by >100-fold. Unfortunately, the present data do not indicate a mechanism for these large cAMP elevations.

Thus, the division of the five muscarinic receptors into two classes (m2 and m4 versus m1, m3, and m5) is not adequate to explain all of their functional properties. This functional division seems to hold for responses observed at low agonist concentrations, but at higher concentrations cAMP increases were observed that do not fit this division. A related phenomenon has been observed in CHO cells, where m2 receptors inhibit adenylate cyclase at much lower agonist doses than those required for stimulation of PI metabolism (22). Taken together, the data emphasize the need to consider the selectivity of receptor coupling to responses in a relative context and the possibility that the same receptor may affect a number of pathways by multiple mechanisms.

Acknowledgments

The authors would like to acknowledge Dr. J. L. Barker and the late Dr. E. Freese for their advice and support and Dr. T. J. Murphy for preliminary experiments. The authors also wish to thank E. A. Novotny and Dr. J. Wess for advice on the functional experiments.

References

1. Kubo, T., K. Fukuda, A. Mikami, A. Maeda, H. Takahashi, M. Mishina, K. Haga, T. Haga, A. Ichiyama, K. Kangawa, M. Kojima, H. Matsuo, T. Hirose, and S. Numa. Cloning, sequencing and expression of complementary DNA encoding the muscarinic ACh receptor. *Nature (Lond.)* **323**:411–416 (1986).
2. Bonner, T. I., N. J. Buckley, A. C. Young, and M. R. Brann. Identification of a family of muscarinic ACh receptor genes. *Science (Washington, D.C.)* **237**:527–532 (1987).
3. Kubo, T., A. Maeda, K. Sugimoto, I. Akiba, A. Mikami, H. Takahashi, K. Haga, T. Haga, A. Ichiyama, K. Kangawa, H. Matsuo, T. Hirose, and S. Numa. Primary structure of porcine cardiac muscarinic ACh receptor deduced from the cDNA sequence. *FEBS Lett.* **209**:367–372 (1987).
4. Peralta, E. G., A. Ashkenazi, J. W. Winslow, D. W. Smith, J. Ramachandran, and D. J. Capon. Distinct primary structures, ligand-binding properties and tissue-specific expression of four human muscarinic ACh receptors. *EMBO J.* **6**:3923–3929 (1987).
5. Bonner, T. I., A. C. Young, M. R. Brann, and N. J. Buckley. Cloning and

MOLECULAR PHARMACOLOGY

Downloaded from molpharm.aspetjournals.org at Universidade do Estado do Rio de Janeiro on December 4, 2012

aspet

expression of the human and rat m5 muscarinic ACh receptor genes. *Neuron* **1**:403–410 (1988).
6. Fukuda, K., H. Higashida, T. Kubo, A. Maeda, I. Akiba, H. Bujo, M. Mishina, and S. Numa. Selective coupling with K^+ currents of muscarinic ACh receptor subtypes in NG108-15 cells. *Nature (Lond.)* **335**:355–358 (1988).
7. Jones, S. V. P., J. L. Barker, N. J. Buckley, T. I. Bonner, and M. R. Brann. Electrophysiological characterization of cloned m1 muscarinic receptors expressed in A9 L cells. *Proc. Natl. Acad. Sci. USA* **85**:4056–4060 (1988).
8. Jones, S. V. P., J. L. Barker, N. J. Buckley, T. I. Bonner, R. M. Collins, and M. R. Brann. Cloned muscarinic receptor subtypes expressed in A9 L cells differ in their coupling to electrical responses. *Mol. Pharmacol.* **34**:421–426 (1988).
9. Neher, E., A. Marty, K. Fukuda, T. Kubo, and S. Numa. Intracellular calcium release mediated by two muscarinic receptor subtypes. *FEBS Lett.* **240**:88–94 (1988).
10. Jones, S. V. P., J. L. Barker, M. B. Goodman, and M. R. Brann. Inositol trisphosphate mediates cloned muscarinic receptor-activated conductances in transfected mouse fibroblast A9 L cells. *J. Physiol (Lond.)* **421**:499–519 (1990).
11. Brann, M. R., B. Conklin, N. M. Dean, R. M. Collins, T. I. Bonner, and N. J. Buckley. Cloned muscarinic receptors couple to different G-proteins and second messengers. *Soc. Neurosci. Abstr.* **14**:600 (1988).
12. Conklin, B. R., M. R. Brann, N. J. Buckley, A. L. Ma, T. I. Bonner, and J. Axelrod. Stimulation of arachidonic acid release and inhibition of mitogenesis by cloned genes for muscarinic receptor subtypes stably expressed in A9 L cells. *Proc. Natl. Acad. Sci. USA* **85**:8698–8702 (1988).
13. Peralta, E. G., A. Ashkenazi, J. W. Winslow, J. Ramachandran, and D. J. Capon. Differential regulation of PI hydrolysis and adenylyl cyclase by muscarinic receptor subtypes. *Nature (Lond.)* **334**:434–437 (1988).
14. Novotny, E. A., and M. R. Brann. Agonist pharmacology of cloned muscarinic receptors. *Trends Pharmacol. Sci.* **4**(suppl.):116 (1989).
15. Felder, C. C., R. Y. Kanterman, A. L. Ma, and J. Axelrod. A transfected m1 muscarinic acetylcholine receptor stimulates adenylate cyclase via phosphatidyl inositol hydrolysis. *J. Biol. Chem.* **264**:20356–20362 (1989).
16. Jones, S. V. P., T. J. Murphy, and M. R. Brann. Physiological comparison of cloned muscarinic receptor subtypes expressed in CHO cells. *Trends Pharmacol. Sci.* **4**(suppl.):116 (1989).
17. Liao, C. F., A. P. Themmen, R. Joho, C. Barberis, M. Birnbaumer, and L. Birnbaumer. Molecular cloning and expression of a fifth muscarinic acetylcholine receptor. *J. Biol. Chem.* **264**:7328–7337 (1989).
18. Buckley, N. J., T. I. Bonner, C. M. Buckley, and M. R. Brann. Antagonist binding properties of five cloned muscarinic receptors expressed in CHO-K1 cells. *Mol. Pharmacol.* **35**:469–476 (1989).
19. Hamill, O. P., A. Marty, E. Neher, B. Sakmann, and F. Sigworth. Improved patch-clamp techniques for high resolution current recording from cells and cell-free membrane patches. *Pflugers Arch.* **391**:85–100 (1981).
20. Fabiato, A., and F. J. Fabiato. Calculator programs for computing the composition of the solutions containing multiple metals and ligands used for experiments in skinned muscle cells. *J. Physiol. (Paris)* **75**:463–505 (1979).
21. Forsythe, I. D., and R. T. Coates. A chamber for electrophysiological recording from cultured neurones allowing perfusion and temperature control. *J. Neurosci. Methods* **25**:19–27 (1988).
22. Ashkenazi, A., E. G. Peralta, J. W. Winslow, J. Ramachandran, and D. J. Capon. Functionally distinct G-proteins selectively couple different receptors to PI hydrolysis in the same cell. *Cell* **56**:487–493 (1989).

Send reprint requests to: Dr. S. V. P. Jones, Neuroscience Research Unit, Department of Psychiatry, Medical Alumni Building, University of Vermont, Burlington, VT 05405.

MOL PHARM
MOLECULAR PHARMACOLOGY
aspet
Downloaded from molpharm.aspetjournals.org at Universidade do Estado do Rio de Janeiro on December 4, 2012